Published in final edited form as:
Biomaterials. 2013 May ; 34(15): 3891–3901. doi:10.1016/j.biomaterials.2013.02.016.

An electrospun scaffold integrating nucleic acid delivery for treatment of full thickness wounds

Serge Kobsa[1,2,3], **Nina J. Kristofik**[1,2], **Andrew J. Sawyer**[1,2], **Alfred L.M. Bothwell**[2,4], **Themis R. Kyriakides**[*,1,2], and **W. Mark Saltzman**[*,1,2]

[1]Department of Biomedical Engineering, Yale University, New Haven, CT 06520

[2]Interdepartmental Program in Vascular Biology and Therapeutics, Yale University, New Haven, CT 06520

[3]Medical Scientist Training Program, Yale University, New Haven, CT 06520

[4]Department of Immunobiology, Yale University, New Haven, CT 06520

Abstract

We developed a multi-functional construct capable of controlled delivery of bioactive substances that can improve wound repair by supporting the intrinsic ability of the skin to heal. We synthesized electrospun scaffolds—composed of a blend of the degradable polymers poly(L-lactide) (PLA) or polycaprolactone (PCL)—that produce highly efficient non-viral *in vivo* gene delivery to cells in the wound bed, provide a protective barrier during early wound healing, and support cell migration and growth. This multi-functional material was tested for its influence on wound healing: scaffolds were loaded with plasmids encoding keratinocyte growth factor (KGF) and applied to full thickness wounds in mice. Compared to scaffolds with control plasmids, animals receiving the KGF plasmid-loaded scaffold produced significant enhancements in wound healing, which was quantified by improvements in the rate of wound re-epithelialization, keratinocyte proliferation, and granulation response. Further, we quantified the expression level of endogenous and plasmid-derived KGF in wound samples: qRT-PCR on wound sections revealed a correlation between the levels of plasmid-derived protein expression and histological analysis of wound healing, revealing an inverse relationship between the expression level of exogenous KGF and the size of the unhealed epithelial layer in wounds. Our findings suggest that engineered nanofiber PLA/PCL scaffolds are capable of highly efficient controlled DNA delivery and are promising materials for treatment of cutaneous wounds.

Introduction

Wound healing is a complex regenerative process of great importance in clinical medicine, controlled by temporal interactions between cells, extracellular matrix components and signaling molecules. Nonetheless, while advances in clinical management and therapeutic modalities have been achieved, serious limitations in the improvement of wound healing

[*]Corresponding authors: Themis R. Kyriakides, Departments of Pathology and Biomedical Engineering, Yale University School of Medicine, 10 Amistad Str. 301C, New Haven, CT 06520, USA, Tel.: +1 203 737 2214, Fax: +1 203 737 2293, themis.kyriakides@yale.edu, W. Mark Saltzman, Department of Biomedical Engineering, Yale University, 55 Prospect Street, New Haven, CT 06511, USA, Tel.: +1 203 432 4262, Fax: +1 203 432 0030, mark.saltzman@yale.edu.

remain, largely due to the complexity of the underlying biology [1-3]. It is widely recognized that a significant improvement in outcomes will come as a result of biologically active therapies for wound healing [4]. A variety of efforts are underway to develop bioengineered skin substitutes to function as “artificial skin.” Unfortunately, because they involve the use of grafted cells, most of these approaches are expensive, labor intensive, present numerous medical and regulatory issues, and results of clinical studies are inconsistent with respect to the efficacy of specific products [5]. As such, there is a need to develop more accessible and efficient advanced therapies for wound healing. One strategy that avoids the aforementioned issues involves controlled delivery of bioactive substances to improve wound healing by supporting the intrinsic ability of the skin to regenerate. Growth factors involved in wound healing, including PDGF, EGF and KGF, are of particular interest given their biological potential [6]. However, barriers to topical use of recombinant proteins include their instability and short half-lives, as well as their limited ability to penetrate into underlying tissues and establish appropriate local tissue concentration gradients. Overall, the clinical use of topical recombinant protein factors has seen only modest success. Specifically, Becaplermin, a PDGF ointment approved by the FDA for treatment of diabetic ulcers, has had a black box warning issued [5,7].

We hypothesized that localized delivery of a DNA plasmid coding for KGF, a crucial growth factor, would overcome these obstacles and lead to significant improvements in wound healing. While this hypothesis is supported by previous reports of growth factor gene delivery to wounds, prior approaches used transfection techniques that are difficult to translate into clinical use, such as viral vectors, ultrasound, liposomes, or electroporation [8-11]. As an alternate, we developed a simple functionalized construct capable of highly efficient, non-viral DNA delivery to the wound, which also provides structural and barrier support needed during the early phase of wound healing.

Materials and Methods

Fabrication of electrospun scaffolds

The electrospinning apparatus was built by arranging a syringe pump with a high voltage source connected to the metal needle tip aimed at a rotating cylindrical collector. 14% w/v solution of poly(L-lactide) (PLA, DURECT) or polycaprolactone (PCL, Sigma) in 3:1 chloroform:acetone solvent was dispersed into a 20 kV electric field and allowed to accumulate on the collector.

Electrospun scaffold seeding and culture

Each 1.5×1.5 cm scaffold was seeded with 2×10^5 3T3 mouse fibroblasts in 0.5 mL of DMEM with 10% FBS and standard concentrations of penicillin and streptomycin. Cells were allowed to attach for 4 hours at 37°C, washed in DMEM, and tra nsferred into fresh medium. The medium was changed every other day.

Physical and mechanical characterization of scaffolds

Cell seeded scaffolds were prepared for SEM using cacodylate buffer and hexamethyldisilazane (Polysciences). Gold sputtering was used prior to viewing on a Philips XL-30 scanning electron microscope (FEI Company). Mechanical measurements and calculated Young’s modulus were obtained using a Model 5948 MicroTester (Instron) according to manufacturer’s protocol.

Evaluation of *in vitro* cell seeding and growth

Efficiency of cell attachment to bare scaffolds was evaluated by measuring the total amount of cellular DNA on scaffolds. Scaffolds were rinsed with physical agitation, cells lysed and

DNA concentration measured using the PicoGreen® dsDNA quantitation reagent (Invitrogen). Cell growth on scaffolds was evaluated using the CellTiter-Blue® cell viability assay (Promega) using a standard curve prepared from the same cells.

Confocal microsocopy

Cell-seeded scaffolds were stained using Alexa Fluor® 594 phalloidin (Molecular Probes, 1:40) and counterstained with DAPI. Images were collected on a Zeiss LSM 510 Meta laser scanning confocal microscope (Carl Zeiss MicroImaging) and processed using Volocity software (Version 5.5.1, PerkinElmer).

Plasmids

pLUC plasmid was from ATCC. pKGF plasmid, in which human KGF gene is expressed in a commercially available blank gWiz™ vector (Genlantis), was constructed and kindly provided by Dr. John Harmon of Johns Hopkins [12-14].

Layer-by-layer DNA loading

Scaffolds were incubated in 0.5 mg/mL PEI (Sigma) solution for 20 minutes, rinsed in sterile DPEC treated water for 1 min and incubated in 0.5 mg/mL DNA solution for 1 hour, followed by another rinse. This cycle was repeated until the desired number of DNA:PEI layers was reached.

Evaluation of DNA loading and release

DNA-loaded scaffolds were degraded in 1M NaOH for 48 hours and then neutralized with H_3PO_4. DNA concentration was measured with PicoGreen®, using a standard curve prepared with NaOH-treated DNA. To investigate the release profile, DNA-loaded scaffolds of known masses were incubated in 500 μL of sterile PBS at 37°C. At appropriate times, PBS was collected and replaced. Released DNA was quantified using PicoGreen®.

In vitro DNA transfection

Scaffolds were loaded with plasmid DNA and seeded with 3T3 cells. Luciferase activity was determined using the Luciferase Assay System (Promega) and a GloMax®-20/20 single tube luminometer. Medium samples were assayed for the amount of secreted KGF using a human KGF/FGF-7 DuoSet ELISA kit (R&D Systems).

Animals

C57BL/6J mice (18-24 g, Jackson Laboratory) were used in accordance with procedures approved by the Animal Care and Use Committees of Yale University, while following the National Institutes of Health Guide for the Care and Use of Laboratory Animals.

Subcutaneous *in vivo* tissue reaction

Six mm circular scaffolds cut using a skin biopsy punch (Acuderm) were implanted into the dorsa of animals in two subcutaneous pockets. After 14 and 28 days, animals were euthanized and the scaffold implants excised together with surrounding tissues for analysis.

In vivo wound experiment

Two symmetrical 6 mm full thickness circular wounds on the dorsa of animals were covered with the appropriate scaffolds, sutured into place using Polysorb 6-0 suture (Covidien). At the appropriate time points, animals were euthanized and the wound area was excised together with the surrounding tissues for analysis.

Histology

Tissues were fixed overnight in Z-Fix (Anatech), embedded in paraffin, sectioned and stained with Masson's Trichrome stain using standard procedures. Histological sections were examined using a Zeiss Axioskop 2 plus microscope.

Histomorphometric measurements

Micrographs consisting of numerous 200X fields of Masson's trichrome stained day 3 and 5 wound sections stitched together using the Image Composite Editor (Microsoft Research) were analyzed using NIH ImageJ. Blinded researchers manually measured the length of the epithelial layer and the *panniculus carnosus* muscle gaps on distance-calibrated images (Supplementary Fig. 1C). Day 7 wound micrographs were processed with ImageJ in order to measure the local thickness of the neo-epithelium (Supplementary Fig. 2) by applying computational methods described previously [15,16].

Ki-67 staining

FFPE wound sections were subjected to heat-mediated epitope retrieval process, followed by staining with rabbit anti-Ki-67 primary antibody (1:100, Abcam) and HRP conjugated donkey anti-rabbit secondary antibody (1:100, Thermo Fisher Scientific). The number of Ki-67 positive cells in a minimum of 5 randomly chosen ×400 high powered fields (HPFs) per section were counted. Care was taken by the blinded researchers to ensure that the HPFs were located in the wound neoepidermis.

Primers

PCR primers were designed to differentially amplify endogenous mouse and plasmid-derived KGF, with details provided in Supplementary Data (Supplementary Fig. 3). Primer candidates were synthesized (Yale Keck Biotechnology Resource Lab) and screened. Data were analyzed using MyiQ Optical System Software, and expressed using the ΔCT method using glyceraldehyde 3-phosphate dehydrogenase (GAPDH) as the reference gene [17].

qRT-PCR

RNA was extracted from FFPE wound tissue samples using RecoverAll Total Nucleic Acid Isolation Kit for FFPE Tissues (Applied Biosystems/Ambion), with cDNA being further synthesized using iScript cDNA synthesis Kit (BioRad) on a Bio-Rad MyiQ Thermal Cycler. Quantitative PCR reaction was carried out using the iQ SYBR Green Supermix (BioRad) on the MyiQ Thermal Cycler.

Statistics

Statistical differences were analyzed using one-, two-, or three-way analysis of variance (ANOVA), as appropriate. *Post hoc* analysis was carried out using Tukey's HSD tests. $P<0.05$ was considered statistically significant.

Results

Electrospun scaffolds support seeding and cell growth *in vitro*

We used electrospinning to produce degradable polyester scaffolds and characterized them for physical and mechanical properties (Fig. 1). Different electrospinning conditions were screened in the scaffold manufacturing process, focusing on several polyesters as scaffold materials: poly(lactic acid) (PLA), polycaprolactone (PCL) and a composite material consisting of 50:50 ratio of poly(lactic acid) and polycaprolactone (PLA/PCL). Electrospun scaffolds were made using all three biodegradable materials under identical conditions.

Tensile stress at yield, as well as tensile stress and strain at both maximum load and break were evaluated for PLA/PCL electrospun scaffolds. Young's modulus of the scaffold was calculated to be 3.2×10^6 N m^{-2}, which is within the range reported for human skin [18,19] (Fig. 1K). These scaffolds support the growth and proliferation of NIH 3T3 mouse fibroblasts. Fluorescence (Fig. 2A-C) and SEM (Fig. 2D-I) imaging of 3T3 cells growing on scaffolds revealed a higher density of cell nuclei on PCL and PLA/PCL scaffolds as compared to the PLA scaffold after a 72-hour *in vitro* culture period. After a 4-hour static seeding period, PCL and PLA/PCL scaffolds showed a strong trend towards being more supportive of cell attachment than the PLA scaffold, and the total cellular content became significantly higher on PCL and PLA/PCL scaffolds compared to PLA scaffolds after a 72-hour culture period (Fig. 2J). Given their favorable physical properties and support of cell attachment and growth, PLA/PCL composite scaffolds were tested in longer term *in vitro* culture, with proliferation detectable on scaffolds over a period of 5 days (Fig. 2K). As expected, once the cells reached confluence on the scaffold, there was a gradual loss of viable cells at 7 days. Visualization using confocal scanning laser microscopy demonstrated three dimensional (3D) cell growth and scaffold infiltration, evidenced by multiple cell nuclei in all three dimensions (Fig. 2L-M), up to the depth of approximately 50 μm (penetration depth limit for confocal visualization in PLA/PCL electrospun scaffolds). Using this approach, 4-6 cell nuclei were visualized in a vertical orientation in the direction of the z-axis.

Functionalized scaffolds deliver DNA to cells

Electrospun PLA/PCL scaffolds were functionalized for controlled delivery of DNA using a layer-by-layer technique to coat fibers in alternating layers of PEI and DNA. The amount of DNA deposited on scaffolds was quantified after varying numbers of DNA:PEI cycles. A direct relationship between the number of DNA:PEI layers and the total amount of DNA on the scaffold was found (Fig. 3A). During the 7 day culture period, a total of 552 ± 16.7 ng of DNA was released from the scaffold into the solution, representing 16% of the total DNA found to be loaded onto the scaffolds. As expected, there was an early period of burst release, followed by release of DNA at a decreasing rate (Fig. 3B). These DNA-layered PLA/PCL scaffolds can transfect 3T3 fibroblasts proliferating on the scaffold, which was demonstrated using a DNA plasmid containing the luciferase reporter gene (pLUC). A direct dose-response relationship between the number of DNA:PEI layers on the electrospun scaffold and the level of luciferase expression was found, which reached significance when scaffolds were loaded with as few as 3 layers of DNA:PEI (Fig. 3C). Importantly, the expression of luciferase persisted for as long as 7 days on electrospun scaffolds *in vitro* (Fig. 3D). Consistent with pLUC transfection, electrospun PLA/PCL scaffolds loaded with a plasmid containing the human KGF gene (pKGF) lead to sustained expression of human KGF by fibroblasts seeded on the scaffolds (Fig. 3E).

KGF gene delivery from scaffolds improves wound healing

To evaluate the tissue reaction to the electrospun composite material, bare, non-DNA-loaded PLA/PCL scaffolds were implanted subcutaneously into the dorsum of mice and explanted after 14 and 28 days. Analysis of histological sections stained with Mason's trichrome revealed minimal tissue reaction developing against the implanted scaffolds. These subcutaneously implanted scaffolds were found to elicit a normal foreign body response, similar to that of other materials that are commonly used in clinical medicine (Fig. 4). PLA/PCL scaffolds were then tested *in vivo* in a mouse full-thickness wound model to investigate their potential clinical utility as functionalized skin substitutes. Six mm circular punch biopsy wounds on the dorsa of mice were covered with PLA/PCL scaffolds loaded with the KGF plasmid DNA and evaluated over a period of 7 days (Supplementary Fig. 1A-B). Wounds treated with KGF plasmid loaded scaffolds were compared to (a) control untreated

wounds, (b) wounds treated with bare PLA/PCL scaffolds, and (c) wounds treated with scaffolds loaded with gWiz plasmid DNA (empty vector with no gene insert). The level of wound closure was determined by measuring the size of the gap in the epithelial layer during re-epithelialization (Supplementary Fig. 1C). Treatment of animals with PLA/PCL scaffolds improved the extent of wound re-epithelialization at days 3 and 5 compared to untreated wounds, regardless of whether the scaffolds were functionalized. Notably, the treatment of wounds with scaffolds functionalized to deliver pKGF DNA further improved the rate of wound closure, which was evident on day 3 in a form of a trend, and became statistically significant by day 5 (Fig. 5A). At day 5, the epithelial gap in pKGF scaffold treated wounds was 65% smaller than in untreated wounds, and approximately 54% smaller compared to non-functionalized scaffolds. As expected, the resulting linear muscle defect present in bisected wound sections gradually decreased as the wound contracted and the panniculus carnosus muscle slowly healed ($p<0.001$) (Fig. 5B). In addition, the presence of a PLA/PCL scaffold lead to a trend towards a smaller muscle defect in wounds, with the addition of pKGF DNA delivery having no effect on the defect size.

PLA/PCL scaffolds lead to more histologically mature wounds

Bisected wound sections stained with Mason's trichrome revealed that scaffold treated wounds displayed more defined and structurally homogeneous granulation tissue at the early time point, with lower levels of leukocytic infiltration and more regular thickening of the epithelium at wound edges compared to untreated wounds (Fig. 5C-F, with schematic in Supplementary Fig. 1D). By day 5 of the healing process, even though the fibrinoid material present in the granulation core of untreated wounds appeared ordered, the structural maturity of both the dermis and the epidermis lagged significantly behind that of wounds treated with PLA/PCL scaffolds (Fig. 5E-F and Fig. 6A-D). The most notable differences were observed in wounds treated with pKGF DNA loaded electrospun scaffolds. In addition to the increased extent of re-epithelialization, the neo-epithelium appeared more structurally mature, with areas of recognizable basal cell layer and stratum corneum (Fig. 5F and Fig. 6D). In fact, even by day 5, dermal recovery and extension of epidermal tongues from the edges of control wounds did not reach the levels seen in pKGF scaffold treated wounds as early as day 3.

pKGF functionalized scaffolds increase neoepidermal thickness

Since virtually all wounds, regardless of treatment, were fully epithelialized a week after injury, the effects of scaffold treatment on the thickness of the resulting epidermal layer were assessed at 7 days. Consistent with the hypothesized effects of pKGF DNA controlled delivery to wounds, treatment with pKGF functionalized scaffolds resulted in a 110% increase in the average thickness of the newly formed epidermal layer (Fig. 7A-C) compared to untreated wounds. The differences in thickness between untreated wounds and the non-functionalized scaffolds were not statistically significant.

Neoepidermal proliferation increases with pKGF delivery

Staining of day 3 and day 5 wound sections revealed a significantly higher number of Ki-67 positive cells in the epidermal layers of wounds treated with pKGF DNA scaffolds compared to those treated with scaffolds delivering blank gWiz vector DNA at both time points (Fig. 7D-F). Interestingly, there were no differences in the overall numbers of Ki-67 positive cells between day 3 and day 5.

Plasmid-derived KGF is expressed in wounds

qRT-PCR reactions on mRNA extracted from formalin fixed, paraffin embedded (FFPE) tissues was used to detect and quantify levels of KGF expression in wounds. To differentiate

endogenously expressed KGF from plasmid-derived KGF, two sets of PCR primers were designed (details in Supplementary Fig. 3). A qRT-PCR reaction using primers specific for plasmid-derived KGF and cDNA from FFPE wound tissue samples resulted in a single 75 bp DNA band corresponding to the expected size of the amplicon (Fig. 8A). It was present only in samples from wounds treated with pKGF DNA releasing scaffolds. Quantification using GAPDH normalization revealed no detectable signal in control tissues, and a robust level of plasmid-derived KGF expression in wounds treated with pKGF DNA functionalized PLA/PCL scaffolds. Notably, levels of expression of plasmid-derived KGF in wounds at different time points were not different, indicating a relatively stable expression of plasmid-derived KGF during the weeklong experimental period.

Presence of scaffolds increases endogenous KGF expression

Expression levels of endogenous KGF were quantified in wound tissue samples using qRT-PCR with primers specific for genome-derived KGF. The expected upregulation of endogenous KGF expression in injured skin was found (Fig. 8B), with a further small increase in endogenous KGF expression in wounds treated with electrospun scaffolds. This increase in endogenous KGF expression was not dependent on DNA functionalization, with no significant differences between bare scaffolds and scaffolds delivering DNA.

Level of plasmid-derived KGF expression correlates with the size of the epithelial gap

Quantification of plasmid-derived KGF in FFPE wound tissues from individual animals using qRT-PCR revealed a moderately strong correlation between level of expression of plasmid-derived KGF and size of the epithelial gap present in that animal (R^2=0.70 at day 3 and R^2=0.77 at day 5). Specifically, there was an inverse correlation, with animals found to have higher levels of plasmid-derived KGF mRNA having smaller epithelial gaps, indicating a direct relationship between pKGF DNA delivery on functionalized scaffolds and higher rates of re-epithelialization (Fig. 8C).

Discussion

We have developed an electrospun nanofiber scaffold capable of efficient non-viral *in vivo* gene delivery to wounds and demonstrated that this approach results in significant improvements in healing of full thickness wounds in the mouse. We chose a PLA/PCL polymer blend because PLA and PCL are both well characterized, non-toxic, and can be used to manufacture scaffolds of the appropriate mechanical characteristics for use in wounds [20-22], resulting in the ease of handling and sufficient mechanical strength to allow the use of sutures. Additionally, the modulus of elasticity of this scaffold falls within the range reported for human skin [18,19], which is an important property in wound dressings and skin replacement constructs as it determines the ability of the construct to conform to the tissue and flex with movement [2].

PLA/PCL nanofiber scaffolds were found to support 3D growth and infiltration of cells, an important finding in the development of a bioactive wound healing construct, as it is well-known that a permissive scaffold is required for fibroblast and keratinocyte ingrowth and migration in wounds - functions typically provided by the provisional matrix of the fibrin clot and, subsequently, granulation tissue [23]. Much like acellular skin substitutes that improve healing [5], our electrospun nanofiber scaffold provides a cell growth permissive matrix.

Scaffolds were shown to support efficient DNA loading using the layer-by-layer technique, in the range of several μg of DNA per mg of scaffold. The layer-by-layer method is a simple, efficient way to surface immobilize significant quantities of DNA based on

electrostatic interactions between negatively charged DNA and a positively charged polyelectrolyte [24-26]. PEI was used as the cationic polyelectrolyte as it has been demonstrated to be safe and to enhance the efficiency of non-viral gene delivery *in vivo* [27,28]. Notably, this work demonstrates the use of the layer-by-layer technique on electrospun scaffolds for *in vivo* applications. Furthermore, it was demonstrated that a direct relationship exists between the number of DNA:PEI bilayers used and the amount of DNA on the scaffold. While ranges from 1 to 7 DNA:PEI bilayers were investigated, it is possible that even greater quantities of DNA could be loaded onto the PLA/PCL scaffold. *In vitro*, DNA was found to be released from the scaffolds with an initial burst phase, a finding consistent with numerous other reports of DNA release from surface immobilized constructs [29] due to the rapid dissolution of electrostatic interactions between polyelectrolytes in aqueous solutions. Burst release of the DNA from the scaffolds in wounds is likely beneficial, as KGF expression is desired early in the course of wound treatment. While it was noted that only 16% of the total loaded DNA was released into solution, we speculate that the DNA remaining on the fibers of the scaffold likely continues to be available for transfection of the cells in contact with the construct.

DNA functionalized scaffolds were found to be efficient at transfection *in vitro*. Again, a direct relationship was established between the number of layers of DNA and transfection of 3T3 fibroblasts with luciferase. It was further found that the expression of luciferase persisted for at least a week *in vitro*. While there was a decrease in the expression level over time, luciferase expression remained robustly detectable. A similar expression profile was found for KGF expression from a plasmid graciously provided by Harmon and colleagues, who developed it and used it to demonstrate an improvement in wound healing following an electroporative transfection of diabetic wounds in mice [11]. As has been discussed, this earlier work provided an important proof of principle, but our method carries the potential for convenience and scale-up for clinical use. We speculate that the transient nature of gene expression resulting from non-viral DNA delivery is clinically beneficial in wound healing, as a temporal local increase in relevant growth factors is desirable until wound closure [30].

Given the known functions of KGF as a keratinocyte mitogen and motogen, and its importance in epithelial repair processes [31], it was expected that the extent and the rate of re-epithelialization by wound keratinocytes would be increased with pKGF delivery from scaffolds. Consistent with this hypothesis, it was found that the treatment of wounds with the scaffolds improved the rate of wound epithelialization by 33% as early as 3 days post injury. We speculate that this trend is due, in part, to the mechanical support that the nanofiber scaffolds provide to the wound and the fibroblast-mediated pro-collagen effects of α-hydroxy acids produced by the breakdown of the PLA/PCL scaffolds [32,33]. In addition, there was a visible trend toward further improvement in wound epithelialization in functionalized scaffolds delivering pKGF. This trend became highly significant by day 5, when pKGF scaffold treated wound openings were as much as 65% smaller than those of untreated wounds as judged by the size of the epithelial gap. Based on these findings, we believe that our scaffolds function synergistically in part both as DNA-delivery-independedent wound dressings, as well as delivery vehicles for the plasmid. The lag in the effect of KGF up-regulation is likely due to the timing of gene expression after transfection, as well as diffusion in the local microenvironment. It is furthermore consistent with what is known about temporal dynamics of the re-epithelialization process, including the time needed for keratinocyte migration and proliferation [34].

We further hypothesized that the mitogenic effects of KGF expression would result in a thicker neo-epidermis at 7 days. Epidermal thickness was measured histomorphometrically by using a computer-based image analysis algorithm capable of measuring the local thicknesses of particular structures [35]. This allowed us to avoid the pitfalls of

measurement bias, especially given the relative complexity and heterogeneity of the neo-epidermis. As expected, treatment of wounds with scaffolds delivering pKGF resulted in a significantly thicker neo-epidermis. This finding is important because, at the relatively early stage of healing a week after injury, a typically thin neo-epidermis can be susceptible to failure and re-injury [36]. Further supporting the hypothesis that pKGF DNA delivery causes increased keratinocyte proliferation and, as a result, improved re-epithelialization, is the finding that staining of tissue sections with Ki-67, a well established marker of proliferation, revealed a significantly higher number of Ki-67 positive cells in the epidermal layers of pKGF DNA scaffold treated wounds compared to the wounds treated with scaffolds loaded with blank gWiz vector plasmids.

To confirm that DNA delivery from nanofiber scaffolds results in gene expression *in vivo*, qRT-PCR was used on mRNA samples extracted from FFPE tissues. Differential primers were designed to separately amplify either the endogenous mouse KGF or the plasmid-derived human KGF. This enabled reliable detection and quantification of the mRNA expression levels in wound samples and also allowed for a direct comparison of protein expression levels and histomorphometric findings, while avoiding technical issues related to immunohistological staining of FFPE sections and their subsequent quantification. In addition to being non-quantitative, because the gene being delivered was one already present in wound tissues, immunohistological staining for KGF would not have allowed for differentiation between the endogenous and the plasmid-derived protein. The presence of KGF mRNA of plasmid origin was visible only in wounds treated with pKGF scaffolds, and it was undetectable in any other wound or skin samples. Furthermore, it was demonstrated that DNA delivery from electrospun PLA/PCL scaffolds was highly efficient, resulting in high and stable levels of gene expression *in vivo* for a period of at least one week. Notably, the level of plasmid-derived gene expression achieved was approximately 10% that of GAPDH, a highly expressed housekeeping gene.

To establish unequivocally that delivery of pKGF from electrospun scaffolds and the resulting increase in KGF expression is the mechanism behind the observed improvements in wound healing, we demonstrated a moderately strong correlation between the pKGF mRNA levels and the size of the epithelial gap in a particular sample, both 3 and 5 days after wounding ($R^2 = 0.70$ and 0.77, respectively). Typically, *in vivo* studies display high variability [37] and, in light of this well characterized phenomenon seen in *in vivo* samples, our results represent a significant finding.

Conclusions

Early epithelialization is known to be one of the most important processes in wound healing, as it helps provide a barrier to fluid and electrolyte loss, as well as preventing infections [38]. Our findings establish a significant biological advantage in wounds treated with pKGF scaffolds. We investigated the effects of this approach on different aspects of the healing process, and demonstrated specific improvements in the rate of wound re-epithelialization, keratinocyte proliferation and granulation response. We were able to reliably detect and quantify the expression level of the biologically relevant protein in wound samples, avoiding the need for extrapolated quantification using reporter gene constructs. Furthermore, the use of qRT-PCR on actual FFPE wound samples enabled us to directly correlate the levels of exogenous protein expression with specific histological findings. The magnitude of improvement in wound re-epithelialization reported here compares favorably with those reported in the literature. There is an improvement in the histological maturity of wounds treated with PLA/PCL scaffolds not reported in many of the previous studies. In addition to advantages over virally-based methods with respect to cost and safety, because our scaffolds are inexpensive, relatively easy to manufacture, and potentially available for coverage of

much larger wounds, they avoid some of the impracticalities and limitations of other non-viral approaches. While our results will need to be validated in other animal models, our findings suggest that engineered electrospun nanofiber PLA/PCL scaffolds capable of highly efficient controlled DNA delivery are a promising bioactive substrate for treatment of cutaneous wounds.

Supplementary Material

Refer to Web version on PubMed Central for supplementary material.

Acknowledgments

We thank Drs. Laura E. Niklason and Christopher K. Breuer for their thoughtful discussions and constructive advice and Elias Quijano for his excellent editor assistance. We are grateful to Prof. John W. Harmon of The Johns Hopkins University School of Medicine for his kind gift of the KGF expressing plasmid. We also thank Dr. Alan Anticevic for his consultation regarding statistical analyses. This research was supported by Yale University Department of Biomedical Engineering Summer Undergraduate Internship Program and by the National Institutes of Health grants NIH EB000487, NIH NS45236, NIH HL085416, NIH DK077910 and NIH MSTP TG T32GM07205. Neither the funding sources nor their representatives were involved in the study design, collection, analysis and interpretation of data, writing of the report, or in the decision to submit this paper for publication.

References

1. Lazic T, Falanga V. Bioengineered skin constructs and their use in wound healing. Plast Reconstr Surg. 2011; 127:75S. [PubMed: 21200276]
2. Boateng JS, Matthews KH, Stevens HNE, Eccleston GM. Wound healing dressings and drug delivery systems: A review. J Pharm Sci. 2008; 97(8):2892–923. [PubMed: 17963217]
3. Gibran NS, Boyce S, Greenhalgh DG. Cutaneous wound healing. J Burn Care Res. 2007; 28(4):577. [PubMed: 17665518]
4. Supp DM. Skin substitutes for burn wound healing: Current and future approaches. Expert Rev Dermatol. 2011; 6(2):217–27.
5. Auger FA, Lacroix D, Germain L. Skin substitutes and wound healing. Skin Pharmacol Physiol. 2009; 22:94–102. [PubMed: 19188757]
6. Barrientos S, Stojadinovic O, Golinko MS, Brem H, Tomic-Canic M. Growth factors and cytokines in wound healing. Wound Repair Regen. 2008; 16(5):585–601. [PubMed: 19128254]
7. Food and Drug Administration. Warning for Regranex - cream for leg and foot ulcers. United States Department of Health and Human Services. 2008
8. Badillo AT, Chung S, Zhang L, Zoltick P, Liechty KW. Lentiviral gene transfer of SDF-1 [alpha] to wounds improves diabetic wound healing. J Surg Res. 2007; 143(1):35–42. [PubMed: 17950070]
9. Alexander MY, Akhurst RJ. Liposome-mediated gene transfer and expression via the skin. Hum Mol Genet. 1995; 4(12):2279. [PubMed: 8634699]
10. Lawrie A, Brisken AF, Francis SE, Cumberland DC, Crossman DC, Newman CM. Microbubble-enhanced ultrasound for vascular gene delivery. Gene Ther. 2000; 7(23):2023–7. [PubMed: 11175314]
11. Marti G, Ferguson M, Wang J, Byrnes C, Dieb R, Qaiser R, et al. Electroporative transfection with KGF-1 DNA improves wound healing in a diabetic mouse model. Gene Ther. 2004; 11(24):1780–5. [PubMed: 15470477]
12. Marti GP, Mohebi P, Liu L, Wang J, Miyashita T, Harmon JW. KGF-1 for wound healing in animal models. Meth Mol Biol. 2008; 423:383.
13. Lin MP, Marti GP, Dieb R, Wang J, Ferguson M, Qaiser R, et al. Delivery of plasmid DNA expression vector for keratinocyte growth factor-1 using electroporation to improve cutaneous wound healing in a septic rat model. Wound Repair Regen. 2006; 14(5):618–24. [PubMed: 17014675]

14. Ferguson M, Byrnes C, Sun L, Marti G, Bonde P, Duncan M, Harmon JW. Wound healing enhancement: Electroporation to address a classic problem of military medicine. World J Surg. 2005; 29:55–9.
15. Hildebrand T, Rüegsegger P. A new method for the model-independent assessment of thickness in three-dimensional images. J Microsc. 1997; 185(1):67–75.
16. Saito T, Toriwaki J. New algorithms for euclidean distance transformation of an n-dimensional digitized picture with applications. Pattern Recognit. 1994; 27(11):1551–65.
17. Schmittgen TD, Livak KJ. Analyzing real-time PCR data by the comparative CT method. Nat Protoc. 2008; 3(6):1101–8. [PubMed: 18546601]
18. Agache PG, Monneur C, Leveque JL, Rigal J. Mechanical properties and young's modulus of human skin in vivo. Arch Dermatol Res. 1980; 269(3):221–32. [PubMed: 7235730]
19. Beumer GJ, Van Blitterswijk CA, Bakker D, Ponec M. A new biodegradable matrix as part of a cell seeded skin substitute for the treatment of deep skin defects: A physico-chemical characterisation. Clin Mater. 1993; 14(1):21–7. [PubMed: 10146446]
20. Chong EJ, Phan TT, Lim IJ, Zhang YZ, Bay BH, Ramakrishna S, Lim CT. Evaluation of electrospun PCL/gelatin nanofibrous scaffold for wound healing and layered dermal reconstitution. Acta Biomater. 2007; 3(3):321–30. [PubMed: 17321811]
21. Powell HM, Boyce ST. Engineered human skin fabricated using electrospun collagen–PCL blends: Morphogenesis and mechanical properties. Tissue Eng Part A. 2009; 15(8):2177–87. [PubMed: 19231973]
22. Blackwood KA, McKean R, Canton I, Freeman CO, Franklin KL, Cole D, et al. Development of biodegradable electrospun scaffolds for dermal replacement. Biomaterials. 2008; 29(21):3091–104. [PubMed: 18448164]
23. Epstein FH, Singer AJ, Clark RAF. Cutaneous wound healing. N Engl J Med. 1999; 341(10):738–46. [PubMed: 10471461]
24. Lu ZZ, Wu J, Sun TM, Ji J, Yan LF, Wang J. Biodegradable polycation and plasmid DNA multilayer film for prolonged gene delivery to mouse osteoblasts. Biomaterials. 2008; 29(6):733–41. [PubMed: 17997482]
25. Jewell CM, Zhang J, Fredin NJ, Lynn DM. Multilayered polyelectrolyte films promote the direct and localized delivery of DNA to cells. J Control Release. 2005; 106(1-2):214–23. [PubMed: 15979188]
26. Sakai S, Yamada Y, Yamaguchi T, Ciach T, Kawakami K. Surface immobilization of poly (ethyleneimine) and plasmid DNA on electrospun poly (L-lactic acid) fibrous mats using a layer-by-layer approach for gene delivery. J Biomed Mater Res A. 2009; 88(2):281–7. [PubMed: 18260146]
27. Huang YC, Riddle K, Rice KG, Mooney DJ. Long-term in vivo gene expression via delivery of PEI-DNA condensates from porous polymer scaffolds. Hum Gene Ther. 2005; 16(5):609–17. [PubMed: 15916485]
28. Scherer F, Schillinger U, Putz U, Stemberger A, Plank C. Nonviral vector loaded collagen sponges for sustained gene delivery in vitro and in vivo. J Gene Med. 2002; 4(6):634–43. [PubMed: 12439855]
29. Ren K, Ji J, Shen J. Tunable DNA release from cross-linked ultrathin DNA/PLL multilayered films. Bioconjug Chem. 2006; 17(1):77–83. [PubMed: 16417254]
30. Branski LK, Gauglitz GG, Herndon DN, Jeschke MG. A review of gene and stem cell therapy in cutaneous wound healing. Burns. 2009; 35(2):171–80. [PubMed: 18603379]
31. Werner S. Keratinocyte growth factor: A unique player in epithelial repair processes. Cytokine Growth Factor Rev. 1998; 9(2):153–65. [PubMed: 9754709]
32. Okano Y, Abe Y, Masaki H, Santhanam U, Ichihashi M, Funasaka Y. Biological effects of glycolic acid on dermal matrix metabolism mediated by dermal fibroblasts and epidermal keratinocytes. Exp Dermatol. 2003; 12(Suppl 2):57–63. [PubMed: 14756525]
33. Bernstein EF, Lee J, Brown DB, Yu R, Van Scott E. Glycolic acid treatment increases type I collagen mrna and hyaluronic acid content of human skin. Dermatol Surg. 2001; 27(5):429–33. [PubMed: 11359487]

34. Broughton G, Janis JE, Attinger CE. The basic science of wound healing. Plast Reconstr Surg. 2006; 117(7 Suppl):12S–34S. [PubMed: 16799372]

35. Dougherty, RP.; Kunzelmann, K-H. Computing local thickness of 3D structures with ImageJ. Microscopy & Microanalysis 2007 Meeting; Ft Lauderdale, FL. 2007.

36. Eccleston, GM. Wound dressings. In: Aulton, ME.; Taylor, K., editors. Pharmaceutics: The science of dosage form design. London: Churchill Livingstone; 2007. p. 264-71.

37. Hanfelt JJ. Statistical approaches to experimental design and data analysis of in vivo studies. Breast Cancer Res Treat. 1997; 46(2):279–302. [PubMed: 9478281]

38. Hunt TK. Basic principles of wound healing. J Trauma. 1990; 30:122. [PubMed: 2328047]

39. Untergasser A, Nijveen H, Rao X, Bisseling T, Geurts R, Leunissen JAM. Primer3Plus, an enhanced web interface to primer3. Nucleic Acids Res. 2007; 35:W71–4. [PubMed: 17485472]

40. Rozen, S.; Skaletsky, H. Primer3 on the WWW for general users and for biologist programmers. In: Krawetz, S.; Misener, S., editors. Bioinformatics Methods and Protocols. Totowa, NJ: Humana Press; 2000. p. 365-86.

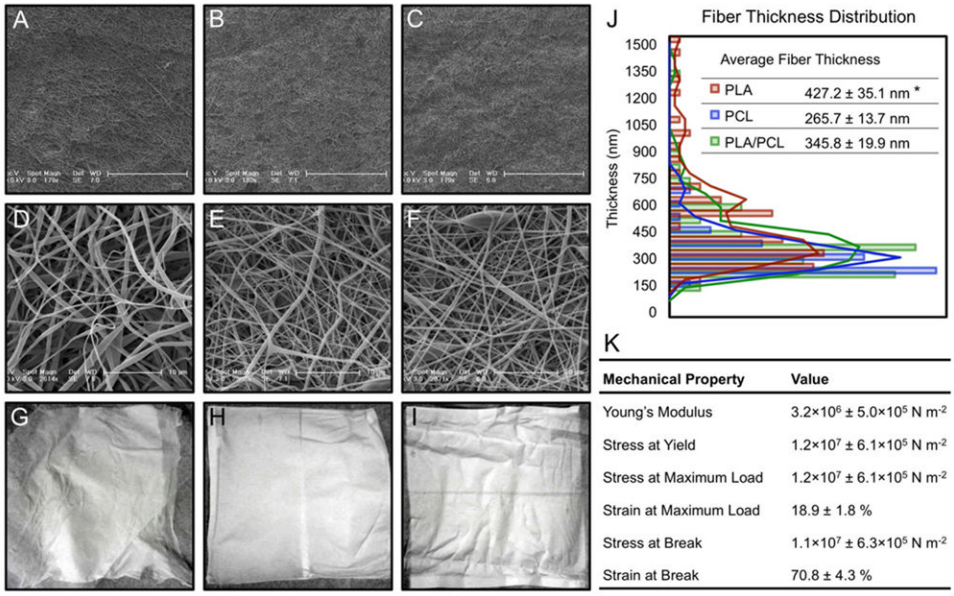

Fig. 1. Development and characterization of electrospun scaffolds

(A-F) In order to investigate their morphology, electrospun scaffolds were visualized using low and high magnification scanning electron microscopy. SEM imaging revealed non-woven structures consisting of randomly deposited polymer fibers of somewhat variable thickness, which resulted in varying porosity in the scaffolds. Morphologically, the fibers appeared smooth, with both linear and curved segments, and occasional randomly distributed areas of bulbous thickening. (G-I) PLA scaffolds were observed macroscopically to have the appearance resembling that of soft cotton with a lint-like surface, and a tendency to separate into horizontal layers. Contrary to PLA, PLC and PLA/PCL scaffolds were smooth to the touch, with a dim luster and no observed layer separation. (J) In addition to the differences observed in the macroscopic appearance and structural morphology between PLA and the PCL-containing electrospun scaffolds, average fiber diameters were also found to differ between the PLA scaffolds (427.2 ± 35.1 nm) and the PCL and PLA/PCL scaffolds (265.7 ± 13.7 nm and 345.8 ± 19.9 nm, respectively) (* $p<0.05$, n=4 per group). (K) Mechanical properties of electrospun PLA/PCL scaffolds.

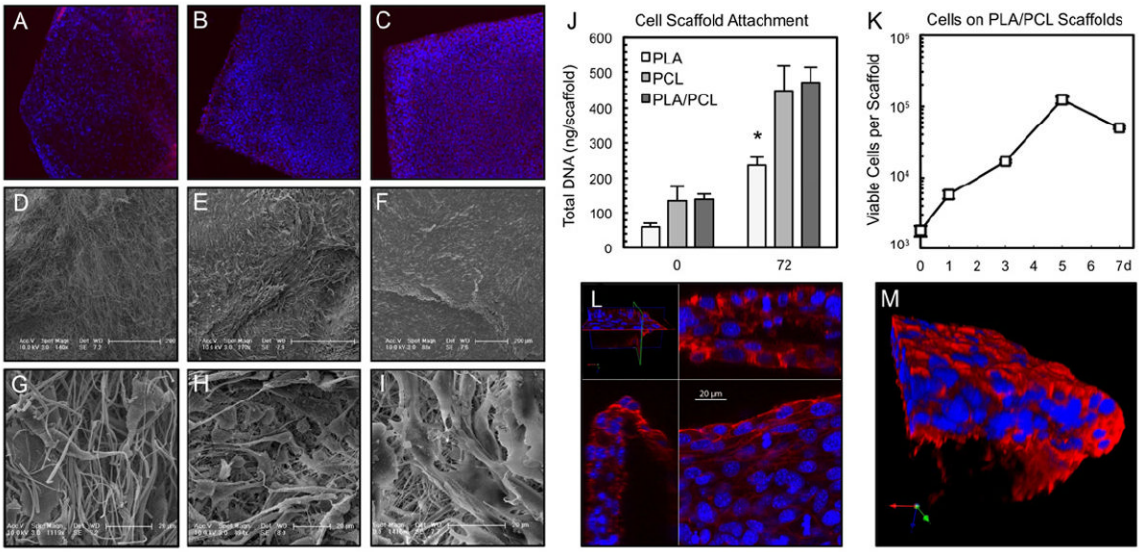

Fig. 2. Electrospun scaffolds support the growth of 3T3 mouse fibroblasts

(A, B, C) Low magnification fluorescent microscopy. (D, E, F) Low and (G, H, I) high magnification SEM. In columns, from left to right are, PLA (A, D, G), PCL (B, E, H) and PLA/PCL composite (C, F, I) scaffolds. The cells form a confluent sheath, seen particularly well on PLA/PCL scaffolds. (J) After a 4-hour static seeding period, PCL and PLA/PCL scaffolds retain approximately twice as many cells as PLA scaffolds, a relationship that is statistically significant after a 72 hour *in vitro* culture period (* $p=0.01$, $n\geq4$ per time point). (K) PLA/PCL scaffolds support long term *in vitro* culture and proliferation of cells (n=5 per time point). A decrease in viable cell numbers occurs by day 7 as the cells reach confluence on scaffolds with a finite surface area (2.25 cm^2). (L) Confocal laser scanning microscopy stack showing cell nuclei growing in multiple layers in all three dimensions on PLA/PCL scaffolds. (M) Rendered reconstruction of cells growing in three dimensions on the PLA/PCL scaffold (edge shown for clarity). Actin in red, nuclei in blue.

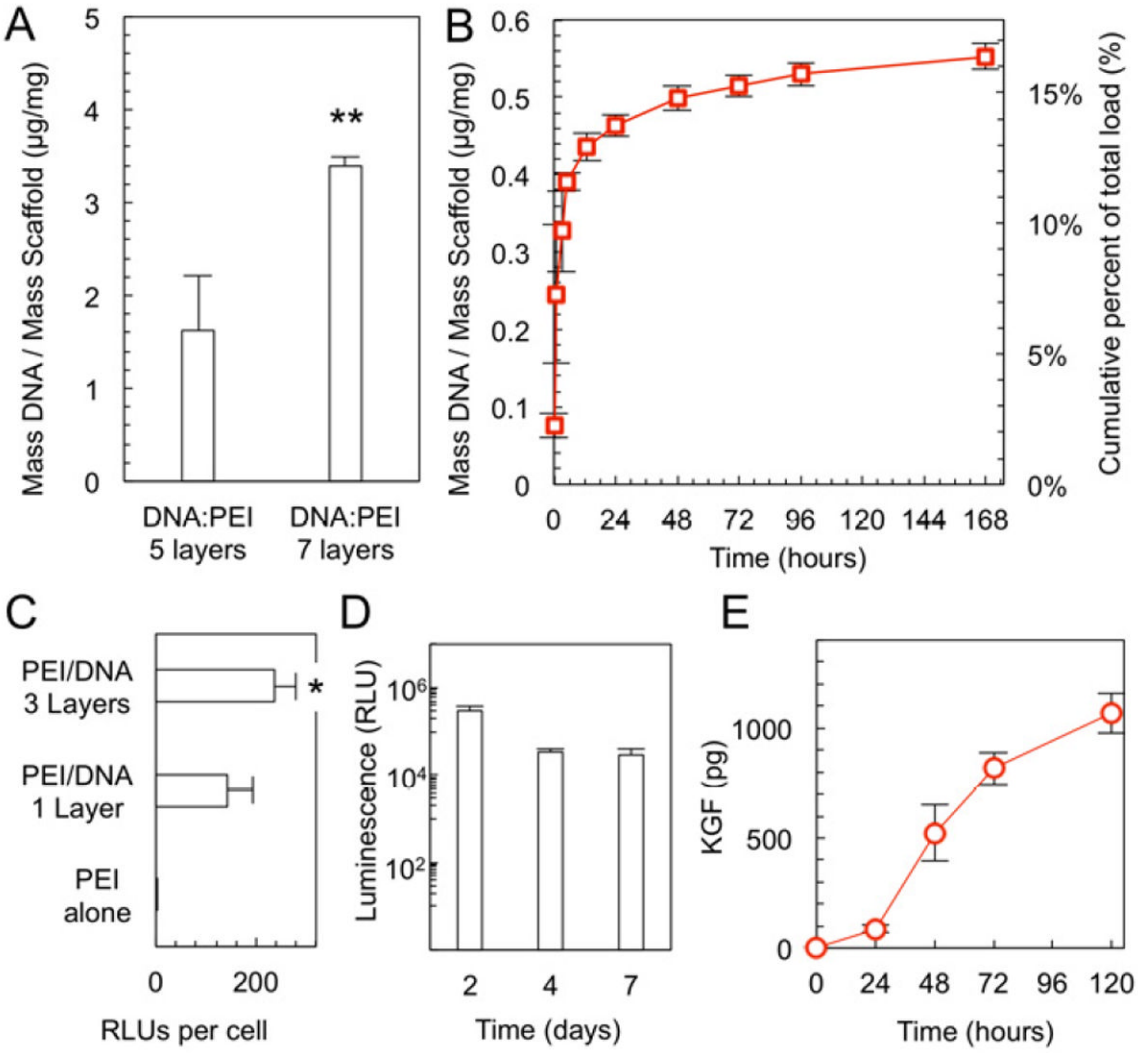

Fig. 3. DNA loading and delivery

(A) Amount of DNA deposited on PLA/PCL electrospun scaffolds using the layer-by-layer technique increases with increasing number of DNA:PEI layers (** p=0.002, n=3). (B) Scaffolds loaded with 7 PEI:DNA layers release the DNA *in vitro* over time (n=3). (C) 3T3 fibroblasts on PLA/PCL electrospun scaffolds take up the pLUC plasmid and exhibit luminescence *in vitro*, commensurate with the number of bilayers (* p=0.02, n=5). (D) Fibroblasts on PLA/PCL scaffolds and layered with pLUC DNA express luciferase over a 7 day period (n=5 per time point). (E) Fibroblasts grown on PLA/PCL scaffolds take up the pKGF plasmid and secrete KGF *in vitro* (n≥4 per time point).

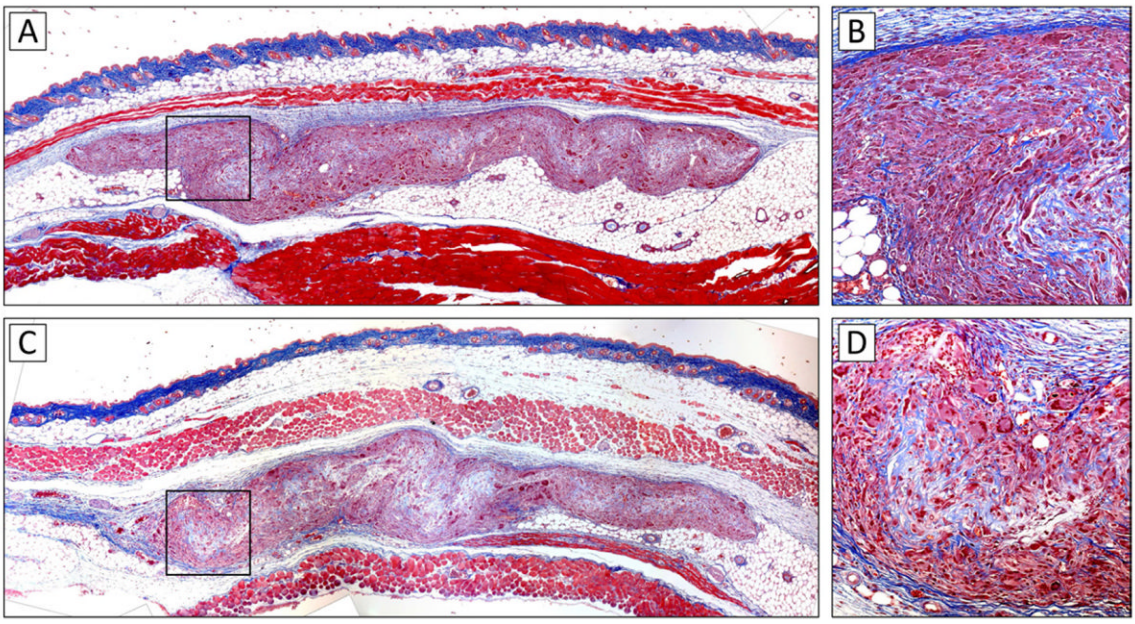

Fig. 4. *In vivo* tissue response to scaffolds

Subcutaneously implanted scaffolds were found to elicit a normal foreign body response, with a collagen capsule visible around the implanted material. Between days 14 (A, B) and 28 (C, D), the density of the implanted scaffolds visibly decreased, consistent with the biodegradable nature of both constituent scaffold materials (PLA and PCL). Consistent with the observation of 3D infiltration of scaffolds *in vitro*, cellular infiltrates were visible throughout the thickness of the scaffolds at high magnification (B, D).

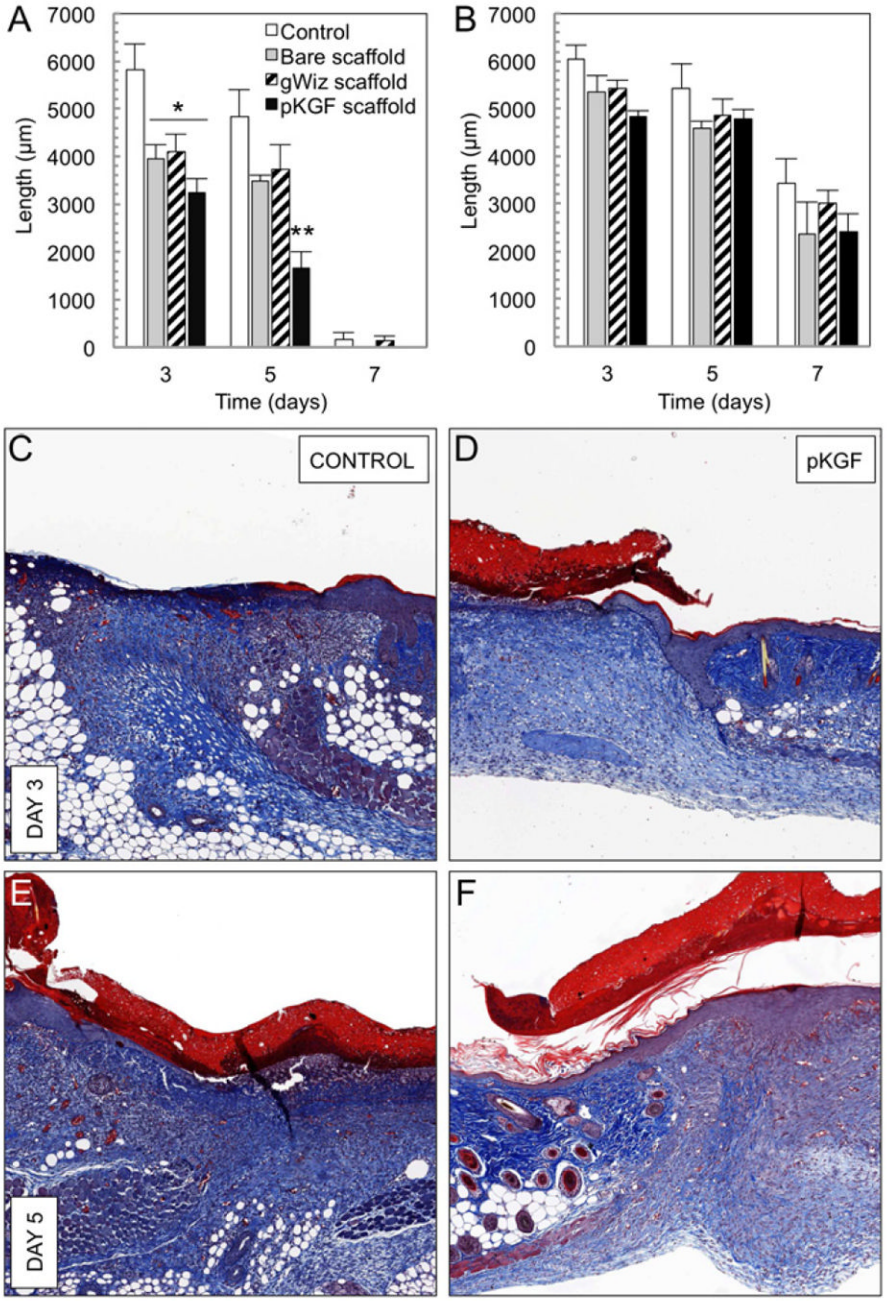

Fig. 5. Effects of scaffolds on wound healing

(A) Effects of scaffolds on the rate of wound re-epithelialization as measured by the length of the epithelial layer gap. At the early time point (day 3), all three scaffolds decrease the epithelial layer gap by approximately 33% compared to control wounds (* $p<0.05$, $n\geq6$ per group), with trend towards further improvement with pKGF delivery. At day 5, treatment with scaffolds delivering pKGF DNA leads to an approximately 65% reduction in the epithelial layer gap (** $p<0.001$, $n\geq5$ per group) compared to untreated wounds and 54% reduction compared to non-functionalized scaffolds ($p<0.03$). (B) The panniculus carnosus defect underlying the wound is statistically unaffected by the presence of a scaffold, regardless of pKGF DNA delivery (n as above). (C through F) Treatment of wounds with

pKGF DNA releasing scaffolds leads to better structural definition and recovery of the dermis, with more significant extension of epidermal tongues from wound edges at both days 3 and 5. Annotated schematic is available in Supplementary Data (Supplementary Fig. 1D).

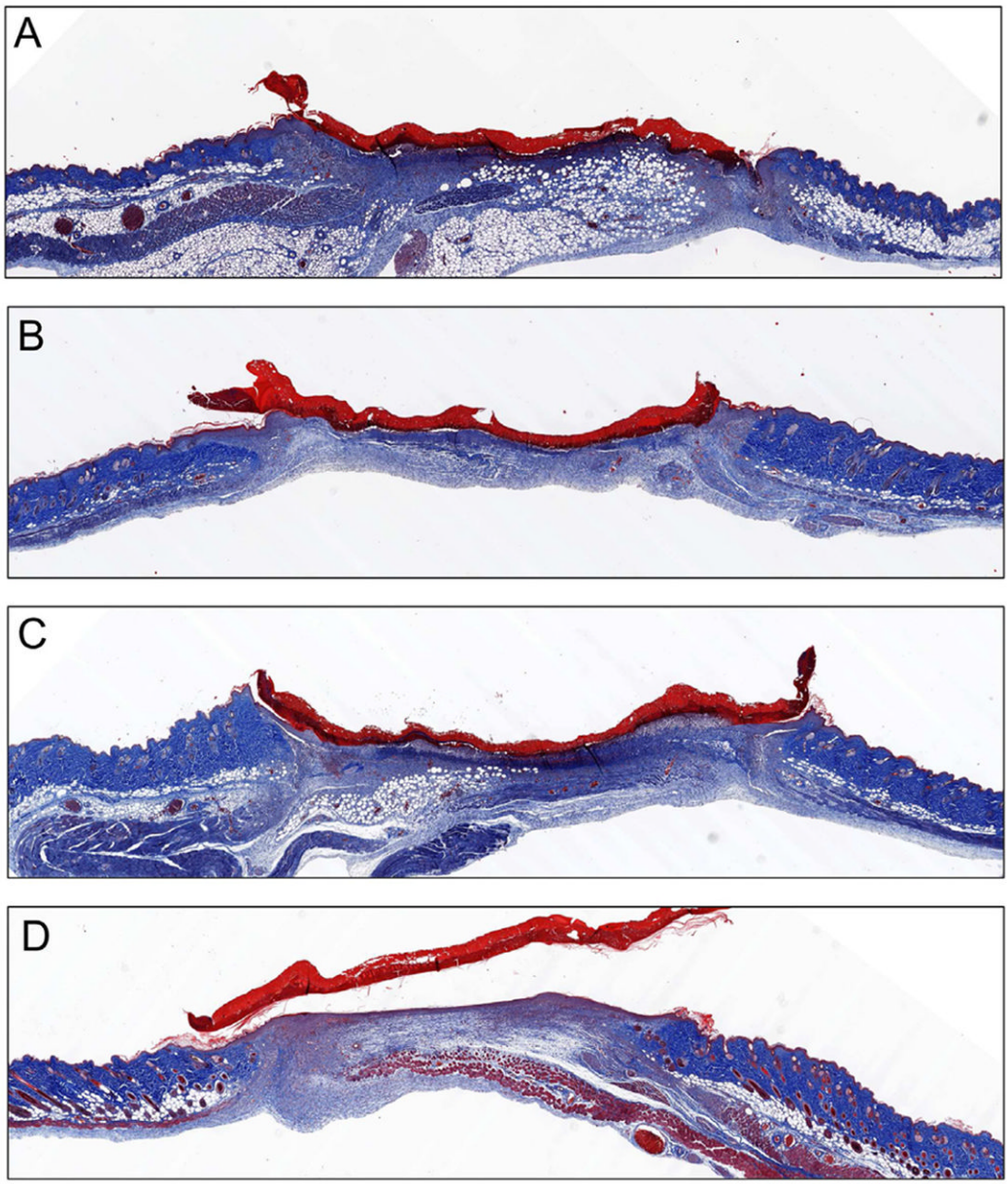

Fig. 6. Histological sections of wounds on day 5

Direct comparison Masson's trichrome stained sections of (A) control, (B) blank scaffold, (C) gWiz empty plasmid and (D) pKGF DNA scaffold treated wounds at day 5 reveals a much higher degree of re-epithelialization and structural maturity of the dermis in pKGF DNA scaffolds as compared to both other scaffolds and untreated wounds.

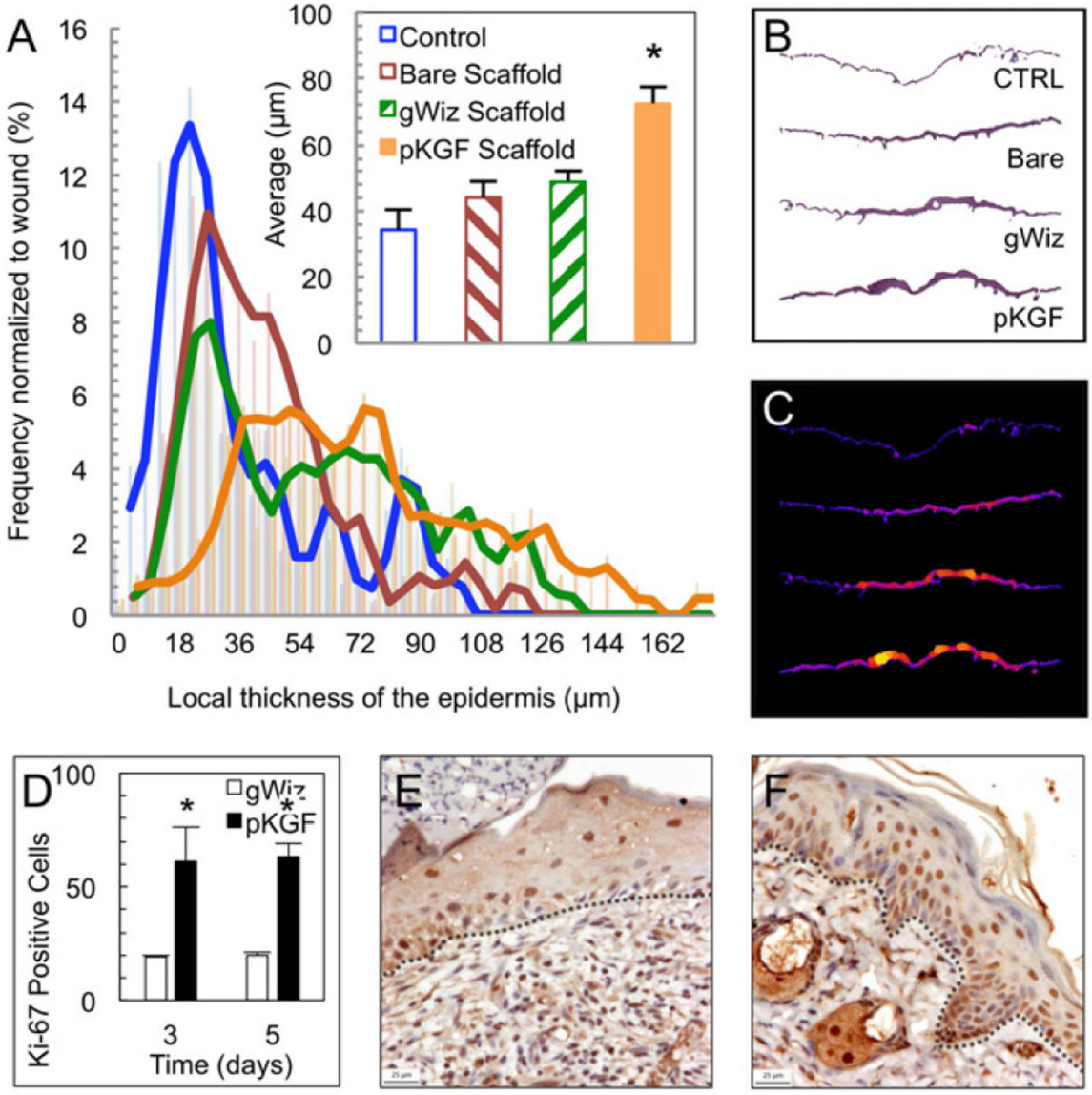

Fig. 7. pKGF functionalized scaffolds increase epidermal thickness and proliferation

(A) pKGF DNA releasing scaffolds lead to an approximate doubling of the average thickness of the epidermis (* p=0.01, n≥3 per group) and the corresponding right shift in the distribution of local epidermal thicknesses in wounds at day 7. Panels illustrate (B) representative epidermal layers and (C) their corresponding computed local thickness maps. (D) A significant increase in the density of Ki-67 positive epidermal cells in the presence of pKGF DNA compared to empty vector DNA (gWiz plasmid) (* p=0.01, n≥3 per time point). Representative histological sections from day 5 of animals treated with (E) gWiz control and (F) pKGF DNA releasing scaffolds. The basement membrane is outlined in black.

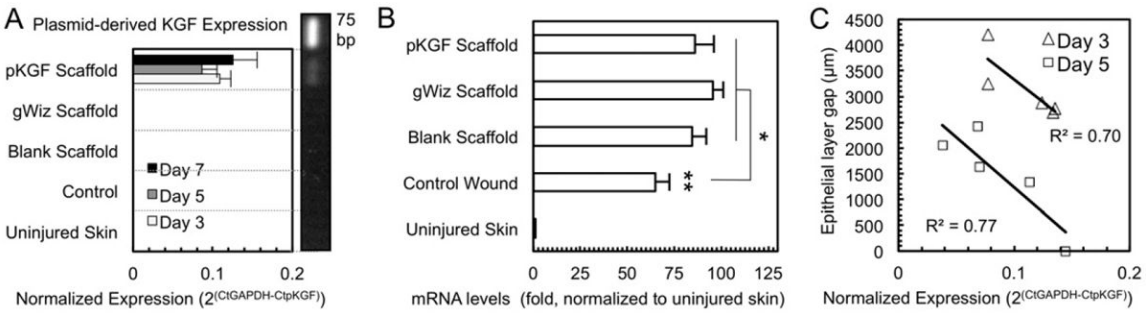

Fig. 8. Detection and quantification of KGF in wound tissues

(A) Plasmid-derived KGF mRNA is only detectable in animals treated with pKGF DNA releasing scaffolds. The expression level of pKGF is relatively stable during the 7 day period ($p=0.47$, $n=5$ per time point). The very bright top band in the vertically oriented gel represents the 75 bp DNA ladder. (B) Day 3 mRNA levels demonstrate an increase in endogenous KGF expression in wounded skin (** $p<0.0001$), with further upregulation of endogenous KGF in all scaffold treated wounds (* $p<0.05$, $n\geq3$ per group). (C) Correlation between the level of plasmid-derived KGF expression and the re-epithelialized area of the wound (epithelial layer gap) at both days 3 and 5. The higher the pKGF expression, the smaller the epithelial layer gap in a given animal ($R^2=0.70$ and 0.77 at days 3 and 5, respectively; $n=5$ per time point).